A SIMPLIFIED METHOD OF AIRFOIL DESIGN

by

Francisco Leme Galvão
Inventory & Production Control Manager,
Embraer, São José dos Campos, Brazil

Presented at the XVIth OSTIV
Congress, Chateauroux, France, 1978

SUMMARY

It is proposed that most already-designed symmetrical airfoil shapes, when taken in non dimensional ordinates, related to their maximum thickness ordinates, can be represented by very simple trigonometric functions.

Using inversely these functions with chosen distinct values for upper and lower surfaces and the uniform load NACA a=1 mean line, it is shown that airfoils for rather different flying conditions can be easily generated.

Some criteria for this choice and examples of airfoils with Stratford-type turbulent recoveries are also presented.

INTRODUCTION

When designing their marvelous flying machines, designers have normally to restrain themselves to the use of published airfoil data.

In this note we will try to normalize and simplify some airfoil basic geometric parameters in order to allow designers to personalize their design by using their own designed airfoils. In doing so, we hope to introduce a mutant gene in the evolutionary selection of the best airfoil for airplanes and gliders provided by actual flying.

SOME BASIC PRINCIPLES

Streamlined shapes are designed to reduce drag, to produce lift or both, as in the case of the airfoil.

Even a flat plate may produce lift if an angle of attack is given to the airstream, but at the expense of high drag, and a curved plate will do the same job with much less drag. The lift comes from the seldom-realized fact that the air being viscous cannot follow around the sharp trailing edge, creating there the so-called Kutta-Joukowsky condition, as viscosity is the origin of both drag and lift. (See Fig. 1.)

Since flying machines have to operate at different speeds and consequently at varying angles of attack, an airfoil nose cannot be sharp as in the case of the leading edge of a vane. Also, an airfoil is supposed to allow for internal structure, fuel tanks, landing gear, controls, etc.

As a result, any subsonic airfoil has the general curved drop shape and although very similar one to another, great differences result from subtle and negligible shape changes. The speed and consequently pressure (Bernoulli Law) variations along the flow over an airfoil surface, are strongly associated with the flow curvature, which near the surface

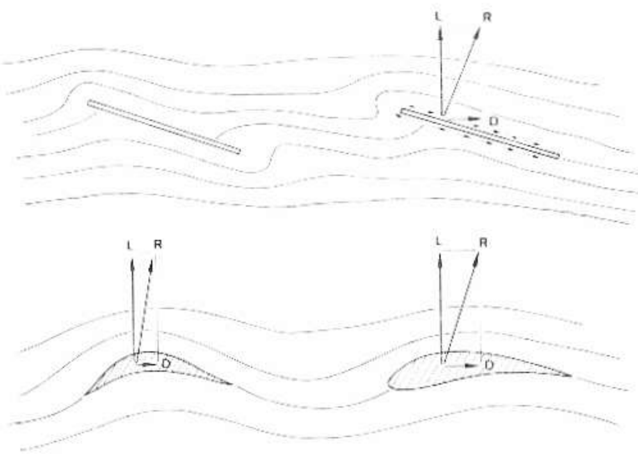

Figure 1.

coincides with the airfoil curvature itself.

The radius of curvature of any curve being a function of its second derivative (Note 1.) we can see why negligible shape variations may give so different flow results.

If now we add over that, the instability and separation flow phenomena occurring in the layers near the wall with all their parameters and complexities, we may think that airfoil design is out of reach of designers, especially of the homebuilder designers having no PHD degree or computer facilities.

However, using all the work already done, we can see that this may not be the case and that with this note, tables, a pocket calculator and good judgement will suffice to obtain a rather good airfoil shape.

DESIGNING SYMMETRICAL SHAPES

Beginning with conformal mapping and going over to computerized prescribed pressure inverse methods, a vast amount of work has been developed and the interested reader may try the reference literature.

Here, we will start dividing the airfoil shape in two rather distinct regions that we will call *nose* and *tail*, separated by the *maximum thickness point*.

In the nose region for small angles of attack the air is normally accelerating, pressure is dropping and a laminar (smooth and parallel) flow may be obtained if allowed by flow Reynolds Number (flow scale) and roughness (surface quality).

At the tail, the air is normally decelerating, pressure is rising and the flow, if not turbulent, will become so (not homogeneously parallel).

Now, for each of these two regions, we will develop *canonical ordinates*, i.e. nondimensional ordinates related to the maximum thickness ordinates x_m, y_m (Note 2.)

Nose Shape

As an airfoil nose shape, even a simple ellipse could be used and some successful old German airfoils had elliptic nose shapes.

However, if we plot in canonical form, rather different airfoils, with different thicknesses and designed by rather different methods arise, and it is amazing to see how near they all fall in a rather close band. Indeed, in a canonical plot it is very difficult to distinguish between an old Joukowsky airfoil and a NACA four- or five-digit airfoil.

Another class is represented by the 63 and 64 low drag airfoils that fall short with Wortmann, Thwaites and other (Ref. 2.) flat top airfoils designed to have maximum low drag range.

Two canonical sets of values are given in the CANONICAL TABLE I and Fig. 1.: One [JK] is computed from the known Joukowsky equation and the other [MR] from harmonic deviation of it fitting a flat top [MR] shapes of Thwaites work. (See Appendix 1.)

The use of trigonometric derived shapes is an assurance that the first and second derivatives and so curvatures, radius, pressures and velocities, will have smooth chordwise variations.

It must be understood that the use of the canonical thickness tables for different x_m and y_m values will not result exactly in the same type of pressure distribution and that also the chosen tail shape will have an influence upon the nose pressure values.

Tail Shape

For the rear part of the airfoil the coincidence in a canonical plot for different airfoils is not as great as for the nose.

However, again, we see that differences are small, with the Joukowsky function falling close in between the NASA laminar 6 digits and Thwaites tails.

Also a historical trend is depicted, start-

Note 1.:

$$c=1/\rho\left[d^2y/dx^2\right] \; / \; \left[1+(dy/dx)^2\right]^{3/2}$$

Note 2.: A correct canonical thickness base should be the ordinates of the maximum velocity point, as in Ref. 12.

ing from the old four-digit convex airfoil tails to more convex-concave (cusped) tails of NASA 6 series. Picking up from Thwaites and Wortmann airfoils to the up-to-date airfoils designed to have Stratford recoveries, such as Strand (Ref. 11) Liebeck (Ref. 12) and Lien (Ref. 13) airfoils.

As Wortmann has already pointed out in his B.S. thesis, pressure distributions afforded by cusped tails are less separation sensitive and result in lower drag. A fact that has been later confirmed by Stratford (Refs. 9 and 3). In his work Stratford established the upper limits of drag reduction and separation avoidance in turbulent pressure recovery, by putting into a differential equation the obvious physical fact that the capability of a flow to be decelerated without separation is proportional to its speed or momentum. (Remember Coanda effect).

Three types of tails are given in the canonical thickness Table 2 and Fig. 1.

One [JK] is again the known Joukowsky function shape. Another [ST] was also obtained from a trigonometric modification of the Joukowsky shape designed to result in a Stratford type recovery canonical pressure distribution for the limit values of x_m/c and y_m/c of fig. 3.

In addition, for tails of simpler construction, a third shape with straight trailing edge [NA] is given computed from the ordinates of a NACA A airfoil tail.

DESIGNING CAMBERED AIRFOILS

The nose and tail canonical thickness presented represent carefully chosen shapes to give some desired pressure distribution characteristics and so much care must be taken to prevent camber from disturbing them.

One of the reasons why Joukowsky airfoils have not been successful (other than the cusped tail construction problem at that time) was that Joukowsky cambered airfoils used a mathematically simple circular camber line that changed adversely their pressure distribution on the lower surface.

There are basically two methods (a third one represents a combination of both) to camber without modifying the pressure distribution of a straight airfoil. First, we can simply camber the airfoil using the known NACA a=1 mean line used in practically all 6 series of laminar airfoils. This mean line besides having the property of producing uniform velocity and pressure changes (of opposite sign) in the upper and lower surface of the airfoil, has also a very simple analytic expression for its ordinates and declivities:

$$y_c/c = \frac{c_{l_i}}{4\Pi}\left[(1-x_c/c)\log(1-x_c/c) + x_c/c\log x_c/c\right] \quad (1)$$

$$\text{arc}\tan\theta = \frac{dy_c}{dx} = -\frac{c_{l_i}}{4\pi}\log\frac{x_c/c}{1-x_c/c}$$

Another simple way of obtaining non-symmetrical airfoil shapes, is to take different thickness values (y_m/c) for the upper and lower surface. (Ref. 6 and 10).

When doing so, a large curvature discontinuity is present in the leading edge and in order to overcome it, it is necessary to introduce a leading edge modification with an osculatory circle resulting in the same leading edge radius for both surfaces. Third, to reduce the inherent pitching moment increase of the first method and the large thickness differences of the second, a combination of both methods seems to be the best compromise to obtain cambered airfoils, this being the method used in this work.

CHOICE OF AIRFOIL PARAMETERS

Now we have reached a critical point in the airfoil design: the selection of the x_m/c and y_m/c values for both airfoil surfaces and the choice between the different canonical shapes.

This choice calls for a good aerodynamic background and a knowledge of the general operating envelope the airfoil is being designed for.

As very general rules, we may say:

- When good finish and accurate construction is possible, the MR-type noses combines with ST-type tails will provide the best performance.

  Fig. 2 presents the computed approximate thickness limit values to be used in function of the "x_o" (position which, as already pointed out, is not coincident with the x_m) and camber c_{l_i}.

  These limits represent the values for which a separation-free Stratford pressure distribution is attained over the airfoil tail for a Reynolds Number of one million, and may be used when designing airfoils for high lift or for maximum thickness minimum drag strut design. (Note 3).

For airfoils operating outside the ideal range of angles of attack, the designer should allow a good margin from these limits to allow for additional angle of attack without separation.

-To avoid the excessively thin ST trailing edges, a JK underside may provide extra tail thickness; and for smaller y_m/c values, the NACA A tail will be useful to obtain feasible trailing edges.

-Higher x_m/c values lead to lower minimum drag but lower ranges of operational angles of attack.

-Whenever construction is not accurate and finish unpolished, the overall JK nose and tail shapes are recommended with corresponding smaller x_m/c values, since laminar flow will not be maintained in the nose.

As an illustrative example of this method, the ordinates, shapes and computed theoretical velocity distribution, as well as drag polars, are given in appendix 3. for six different air foils designed for six different purposes:

A. -72MRST3616/JKNA 5206
A hang glider airfoil designed to have a large $c_{l_{max}}$ value with plenty of thickness for low constructional weight and reasonable drag, at low Reynolds Numbers.

B. -36MRST 4012/MRJK 4807
A glider airfoil intented to have a high L/D with a large low drag range at high c_l values and reasonable $c_{l_{max}}$ without flaps.

C. -18MRST 4408/MRJK 4408
Subsonic airplane airfoil designed to have small drag at low c_l with low c_m.

D. -36JKNA4804/MRST 4408
High subsonic airplane airfoil designed to have the smallest upper surface velocities with lift sufficient for high speed flight without separation at the lower surface.

E. -00JK3510/JKNA4004
Homebuilder airplane airfoil - designed to have low construction sensitivity, reasonable drag and maximum lift values, small pressure center travel (low $c_{m_{a.c.}}$) and simplicity of curves.

Note 3: As shown on appendix 2, RN effects on Stratford flows are small ($RN^{1/5}$) and so one million is conservative.

F. -18JK3512/JKNA4004
Homebuilder glider airfoil - same as above but for higher c_l values.

USING THE TABLES

Once the desired values for camber c_{l_i}, x_m/c and y_m/c have been chosen for both upper and under surface, the airfoil ordinates may be determined. The thickness airfoil ordinates (x_t/c) and (y_t/c) are obtained from canonical tables 1 and 2. For the nose:

$$x_t/c = x_m/c \;.\; x/x_{m\,(1)} \qquad (3)$$

$$y_t/c = y_m/c \;.\; y/y_{m\,(1)} \qquad (4)$$

and for the tail:

$$x_t/c = x_m/c + (1-x_m/c)\left(\frac{x-x_m}{c-x_m}\right) \qquad (5)$$

$$y_t/c = y_m/c \;.\; y/y_{m\,(2)} \qquad (6)$$

Using equation (I) and (II) the camber ordinate and declivicy values y_c/c and θ are obtained for each x_t/c computed above. Now the airfoil coordinates are obtained by the well-known relations:

$$x/c = x_c/c \pm y_t/c \sin\theta \qquad (7)$$

$$y/c = y_c/c \pm y_t/c \cos\theta \qquad (8)$$

Using a programmable pocket calculator, such as an HP-25, a new airfoil is born every 30 minutes. The osculatory nose radius is obtained as shown in Appendix 1.

REMARKS

The presented method being a simplified one as it is, does not afford the possibilities of the sophisticated computer step by step airfoil methods. Notwithstanding, for x_m/c and y_m/c values within 0.3 to 0.5 and 0.6 to 0.15 respectively, good airfoils may result, but they will hardly outmatch a carefully designed airfoil, unless by chance.

Another point to be remarked is that at the x_m stations all airfoils designed by this ethod will present curvature discontinuities (excepting the JK airfoils with x_m/c = 0.25).

In consequence, in all airfoils the laminar to turbulent transition in the boundary layer will tend not to go beyond that point, irrespective of Reynolds Number and angle of attack. With airfoils designed with the MR nose and the strongly cusped Stratford tails, if Reynolds Numbers and angle of attack are such that could force transition behind the x_m/c point, it is extremely likely that a laminar separation will result with strong adverse effects on lift and drag.

Since the method does not allow introduction of corrections like the Wortmann instability ranges to start the transition before the strong adverse Stratford pressure gradient the use of less sophisticated but also effective physical transition inducers is recommended, such as a trip wire or a step ~5% ahead of x_m/c point, whenever the designer feels or detects that laminar separation is at stake.

Finally, a practical advice for laying-up airfoil drawings, templates, jigs or also for designing wing-structures, such as ribs and skins.

We have seen that d^2y/dx^2, second derivatives (or curvature) discontinuities have the deleterious effects on airfoil pressure distribution and therefore on airfoil performance. Well, from strength of materials theory, we know that an elastic beam deflection is determined by:

$$\frac{d^2y}{dx^2} = M/EI$$

where M is the bending moment on the beam

E "Young's modulus"

I beam inertia

So, elastic beams without bending moments or inertia discontinuities have smooth curvatures and those with discontinuities, generated by concentrated loads on support and section changes, have not.

With this fact in mind, a smart designer can obtain much better results from a poorer airfoil than a poor designer from an up-to-date computer-generated airfoil, but traced through the right points with poor French curves.

A last remark is associated with the need for using a single leading edge radius for both upper and lower surfaces.

Wind tunnel tests with double thickness method cambered airfoils (Ref. 6) have shown that the double radius discontinuity at the leading edge affects the stagnation point location and has disastrous consequences on airfoil drag due to distortions introduced in the under surface pressure distribution and boundary layer transition.

And so please.... never use French curves, unless you are in Paris.

REFERENCES

1. IRA ABBOTT & ALBERT VON DOENHOFF
Theory of Wing Sections-Dover Publications 1949.

2. B. THWAITES
A new family of low drag wing with improved c_l Ranges. Research & Memoranda No. 2292, ARC Technical Report, 1950

3. B. S. STRATFORD
The prediction of separation of the turbulent boundary layer.
Journal of Fluid Mechanics, Vol 5, 1958.

4. RIEGELS
Aerodynamische Profile.

5. F. L. GALVÃO
A new look at old airfoils.
OSTIV Publication VIII, June 1965.

6. F. L. GALVÃO
Theoretical and experimental study of mean line effects over two-dimensional laminar airfoils.
I.T.A. Master Thesis 1970.

7. LAGARDE ET J. P. DE LOOF
Etude et essais de profils laminaires.
L'Aeronautique et Astronautique, No. 32, 1971.

8. GEORGE S. PICK AND DOUGLAS LIEN
The development of a two-dimensional high endurance airfoil - NASA - CR 2315, James Nash-Webber, 1972.

9. F. X. WORTMANN
A critical review of the physical aspects of airfoil design at low Mach numbers.
NASA CR 2315, James Nash-Webber, 1972.

10. F. L. GALVÃO
Some thoughts on Nature and Sailplane Design. OSTIV Publication No. XII, July 1972.

11. T. STRAND
Exact Method of designing airfoils,
Journal of Aircraft, Vol. 10, No. 11, November 1973.

12. A. M. O. SMITH
High Lift Aerodynamics
Journal of Aircraft, Vol. 12, No. 6, June 1975.

APPENDIX I

Canonical shape computation:

The known Joukowsky airfoil shape is given by:

$$x = \frac{c}{2}\,(1 + \cos\theta)$$

$$y = \xi \sin\theta\,(1 - \cos\theta)$$

where maximum thickness for $\theta = 120^0$ where

$$x_m = 0.25c$$

$$y_m = 1.29904 \times \xi$$

Therefore, the canonical expression we have in the nose

$$\frac{x}{x_m} = 2\,(1 + \cos\theta)$$

$$y_1/y_m = 0.76980 \sin\theta\,(1-\cos\theta)$$

To obtain the MR shape, the difference in the canonical shapes of the Thwaites MR 45020 airfoil and the Joukowsky airfoil was analyzed harmonically and the following correction to y/y_m was obtained:

$$\Delta y/y_m = \frac{\sin 6\theta}{48} + \frac{\sin\theta'(\cos\theta'-1)}{18}$$

where

$$\theta' = \text{arc cos}\,(3+4\cos\theta)$$

For the tail, the Joukowsky airfoil becomes in canonical shape:

$$\frac{x-x_m}{1-x_m} = \frac{1}{3}\,(1+2\cos\theta)$$

and the same as for the nose

$$y_2/y_m = 0.769800 \sin\theta\,(1-\cos\theta)$$

As for the nose, to obtain the correction for Stratford tails a numerical harmonic analysis of difference was made, using this time the differences in canonical shapes between the Joukowsky and the mean line of the Pick & Douglas airfoil, (Ref. 8) designed to have a Stratford flow with the highest possible camber, obtaining:

$$\Delta y/y_m = -\frac{1}{6} \sin 4\theta'' - \frac{1}{48} \sin\theta''' \quad \text{where}$$

$$\theta'' = \text{arc cos}\,\frac{1}{3}\,(4\cos\theta-1) \quad \text{and}$$

$$\theta''' = \frac{2\pi}{3}\,(1+2\cos\theta)$$

A numerical evaluation of the limit when $x/x_m \to 0$ of the curvature

$$c = 1/\rho = \left|d^2y/dx^2\right| \;/\; \left[1+(dy/dx)^2\right]^{3/2}$$

of the canonical nose shapes, gives the following numerical results:

$\rho = K y_m^2/x_m$ with $K = 1.3200$ for JK noses and $K = 0.8056$ for MR noses

For different thicknesses cambered airfoils we can write for the osculatory leading edge radius:

$$\rho = 0.5\,(K_u y_{mu} + K_l y_{ml})^2 \,/\, (K_u x_{mu} + K_l x_{ml})$$

where u and l subscripts refer to upper and lower surfaces.

TABLE I - Nose Canonical Ordinates

x/x_m	(y/y_m) 1	
	JK	MR
.007611	.133930	.104348
.030384	.265318	.210929
.068148	.391689	.318672
.120615	.510696	.429010
.187384	.620182	.539299
.267949	.718233	.646185
.361696	.803227	.745488
.467911	.873870	.832913
.585786	.929231	.904723
.714415	.968754	.958131
.852847	.992271	.991103

TABLE 2 - Tail Canonical Ordinates

θ	$\frac{x-x_m}{c-x_m}$	y2/Ym		NACA A	
		(JK)	(ST)	$\frac{x-x_m}{c-x_m}$(NA)	y2/Ym(NA)
115	.051588	.992526	.979508	.08333	.9956
110	.105320	.970784	.934305	.16667	.9692
105	.160787	.936020	.869822	.25000	.9204
100	.217568	.889749	.792069	.33333	.8524
90	.333333	.769800	.620071	.41667	.7696
80	.449099	.626461	.456682	.50000	.6751
70	.561347	.475966	.322113	.58333	.5709
60	.666667	.333333	.219688	.66667	.4601
50	.761858	.210649	.143646	.75000	.3464
40	.844030	.115765	.086854	.83333	.2324
30	.910684	.051567	.045011	.91667	.1183
20	.959795	.015878	.017114	1.00000	.0043

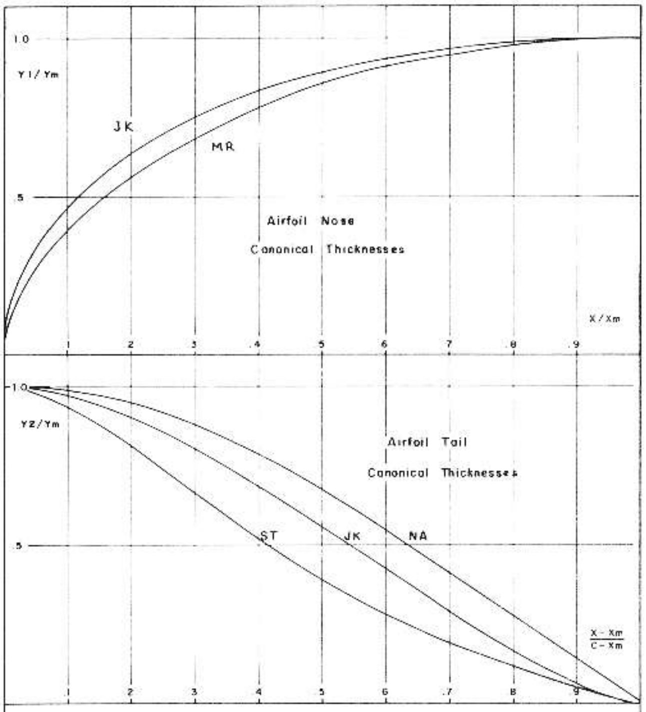

FIG. -1-

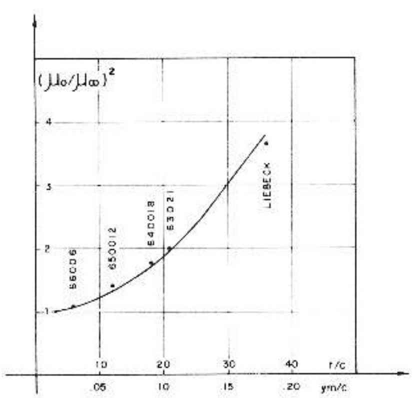

FIG -2-

$(Vm/V\infty)^2$ "Roof top" velocities for diferent thicknesses.

$V/Vm \sim \left[1 + 22.676\ (t/c)^2\right]^{1/2}$

APPENDIX II

Determination of approximate limits of Stratford pressure recoveries in airfoil tails.

According to Ref. 3 & 12, the Stratford flow, in which the margin of separation is zero everywhere, has the pressure distribution:

$$\overline{C}_p = 0.645\ \{0.435\ R_o^{0.2}\ [(x/x_o)^{0.2} - 1]\}^{1/3}$$

for $\overline{C}_p \leq 0.5714$ (for $\overline{C}_p = 1 - (V/V_o)^2$) and

$$\overline{C}_p = 1 - a/[(x/x_o) + b]^{1/2} \text{ for } \overline{C}_p \geq 0.5714$$

the point for which $\overline{C}_p = 0.5714$ is:

$$x^*/x_o = \left(1 + \frac{1.5983}{R_o^{0.2}}\right)^5 \text{ where}$$

$$\frac{d\overline{C}_p^*}{dx/x_o} = \frac{0.0430\ \{0.435\ \ R_o^{0.2}\}^{1/3}}{(x^*/x_o)^{0.8}[(x^*/x_o)^{0.2} - 1]^{2/3}}$$

thus,

$$b = \left[\frac{0.2143}{(d\overline{C}_p^*/dx/x_o)}\right]^{1/2} - x^*/x_o$$

and

$$a = 0.4286\ [b + x^*/x_o]^{1/2}$$

For an airfoil with "rooftop" nose and Stratford pressure recovery in the tail we can write that at the trailing edge we have

$$\overline{C}_{p_{te}}\ \text{min} = 1\ \left(\frac{U_{te}}{U_o}\right)^2 \quad \text{or}$$

$$= 1 - \left(\frac{U_{te}/U_\infty}{U_o/U_\infty}\right)^2$$

U_{te} = trailing edge velocity and

U_o = "roof top" nose constant velocity

From various rooftop airfoils with maximum thickness around 40% chord we can estimate the rooftop velocity as: (see Fig. 2)

$$\left(\frac{U_o}{U_\infty}\right)^2 \cong 1 + 23\ (t/c)$$

and trailing edge velocity as:

$$\left(\frac{U_{te}}{U_\infty}\right) \cong .92$$

and for a = 1 mean line cambered airfoils:

for c_{l_i} = .4 (U_{te}/U_∞) = 1.020

for c_{l_i} =.8 (U_{te}/U_∞) = 1.120

With the above estimated values and previous analytical expressions, we can estimate for each Reynolds Number, and for each roof top position x_o/c, the maximum thickness with separation free flow for angles of attack within the rooftop or laminar bucket of the airfoil.

In table 3 and Fig. 3 these values are presented for a chord line Reynolds Number of one million.

When using these data it must be kept in mind that for MR and ST canonical thickness the rooftop length, as already shown, is not coincident with x_m, but is approximately $x_o \sim x_m + 0.50\, y_m$.

x_o/c	C_{pte} min	c_{l_i}=0		c_{l_i}=0.4		c_{l_i}=0.8	
		(U_o/U) max	(y_m/c) max	(U_o/U) max	(y_m/c) max	U_o/U max	y_m/c max
.25	.7614	1.8836	.166	2.0882	.191	2.2929	.215
.35	.7097	1.7076	.144	1.8933	.167	2.0789	.190
.45	.6597	1.5772	.127	1.7486	.150	1.9201	.171
.55	.6067	1.4669	.112	1.6264	.134	1.7858	.154

Table 3 - Limit values of trailing edge C_{pte}, roof top velocities and y_m/c Stratford turbulent recoveries and Reynolds Number=1,000,000.

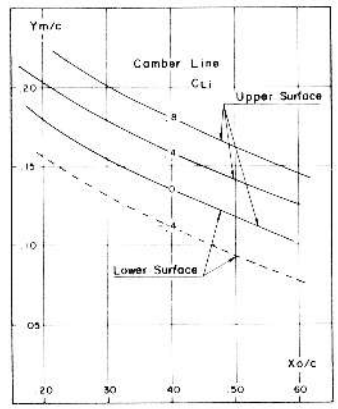

Fig. 3
Approximate limits for Ym/c
for a Stratford flow with
turbulent rooftop up to X=Xo
RN = 1 x 10^6

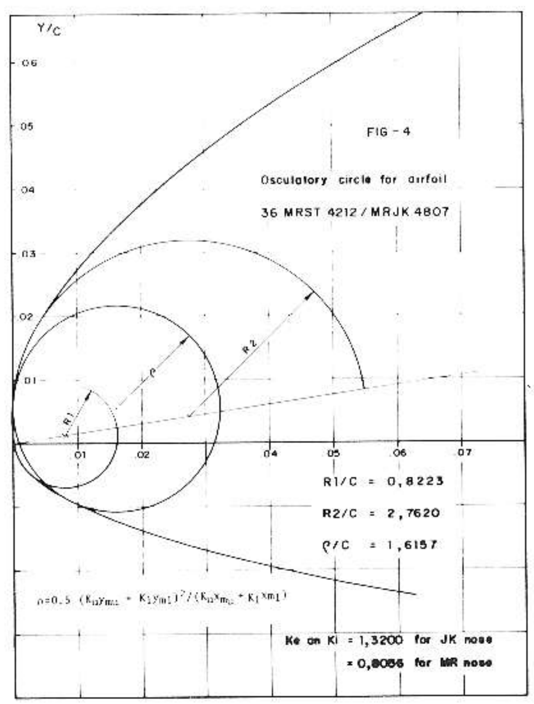

APPENDIX III

Airfoil nomenclature, ordinated and characteristics.

Using the canonical tables 1 and 2 of Appendix I, the ordinates of the six airfoils were calculated from their main geometrical parameters shown by their nomenclature, which completely defines each airfoil as follows:

BR KK AABBNNMM / CCDDXXYY where

BR - Indicative of the family (Brazilian).
KK - Design c_lx100 of the NACA a=1 *camber* line used (it is not a *mean* line, unless MM=YY).
AA - Upper surface nose type indicative letters.
BB - Upper surface tail type indicative letters.
NN - Upper surface x_m/c x 100.
MM - Upper surface y_m/c x 100.
CC - Under surface nose type indicative letters.
DD - Under surface tail type indicative letters.
XX - Under surface x_m/c x 100.
YY - Under surface y_m/c x 100.

The chosen six airfoils ordinates were then fed to a FORTRAN computer program using the Riegels numerical methods (Ref. 4) to obtain the velocity distributions and c_l, c_d coefficients for various angles of attack. Also theoretical values for $dc_l/d\alpha$, $\alpha_{c_l=0}$, $c_{m_{ac}}$, and c_{l_i} were computed.

It is important to remark that drag coefficients were computed without quadrature Schlichting expressions, supposing the transition to occur on computing station after maximum velocity point, on both surfaces for normal case and at x/c = 0.0169 for the turbulent case.

Also fully attached flow was assumed and so drag values outside low drag range or for c_l values far from c_{l_i} should be cautiously regarded.

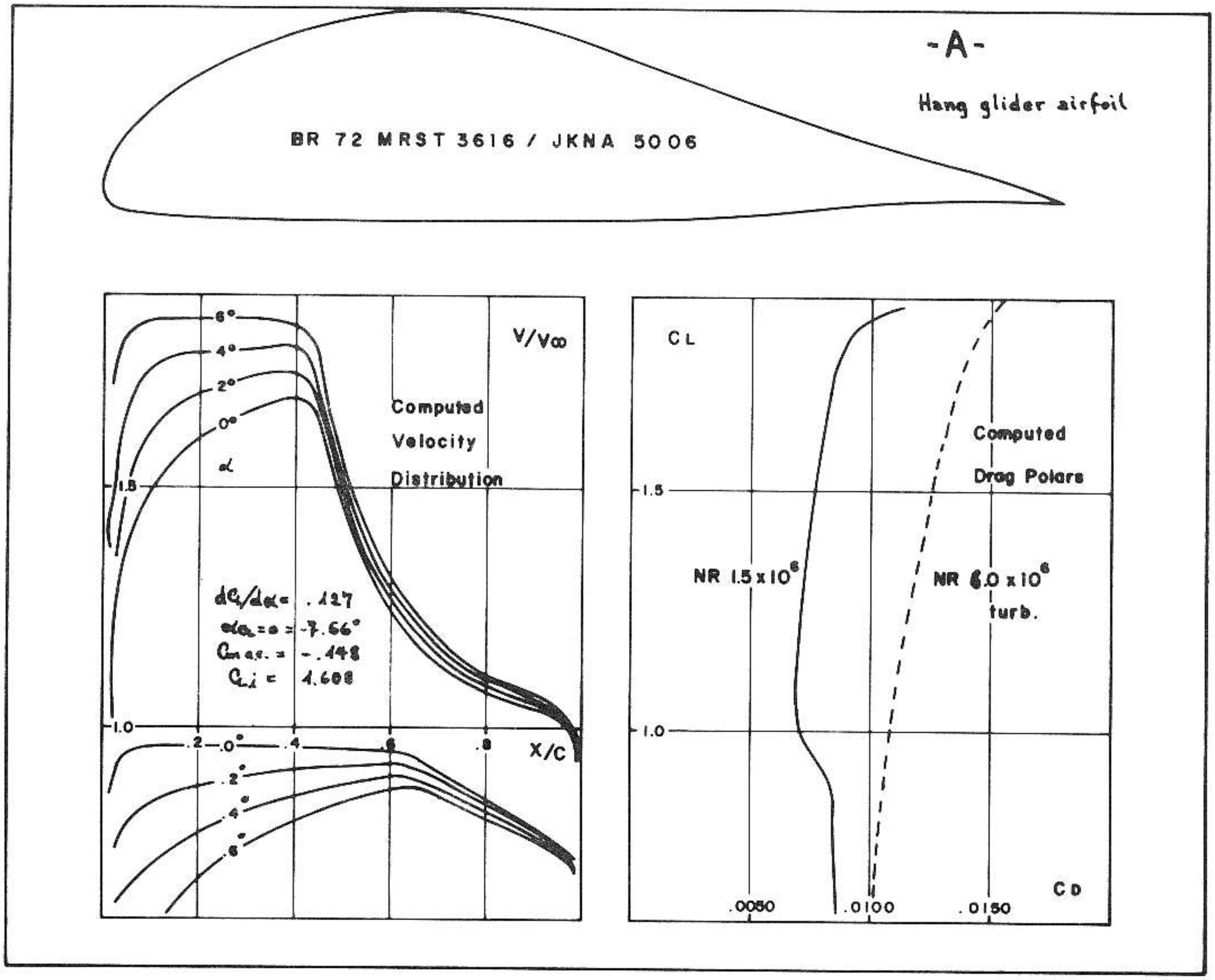

A - AIRFOIL 72MRST3616/JKNA5006
FOR HANG GLIDERS

UPPER SURFACE		UNDER SURFACE	
-0.264	1.690		
0.266	3.609	1.892	-1.094
1.393	5.652	3.854	-1.450
3.136	7.789	6.510	-1.712
5.453	9.957	9.852	-1.895
8.322	12.085	13.859	-2.011
11.721	14.089	18.503	-2.073
15.622	15.887	23.754	-2.091
19.989	17.407	29.573	-2.078
24.783	18.592	35.918	-2.047
29.958	19.400	42.744	-2.015
35.469	19.763	50.000	-1.999
38.909	19.535	54.109	-1.993
42.488	18.886	58.221	-1.894
46.171	17.901	62.337	-1.702
49.922	16.674	66.462	-1.437
57.502	13.858	70.597	-1.128
64.989	11.048	74.744	-0.797
72.206	8.573	78.903	-0.462
78.931	6.497	83.078	-0.148
84.985	4.751	87.268	+0.109
90.193	3.253	91.474	+0.275
94.399	1.975	95.707	+0.301
97.483	0.958	100.000	+0.026

Osculatory leading edge radius = 2.279

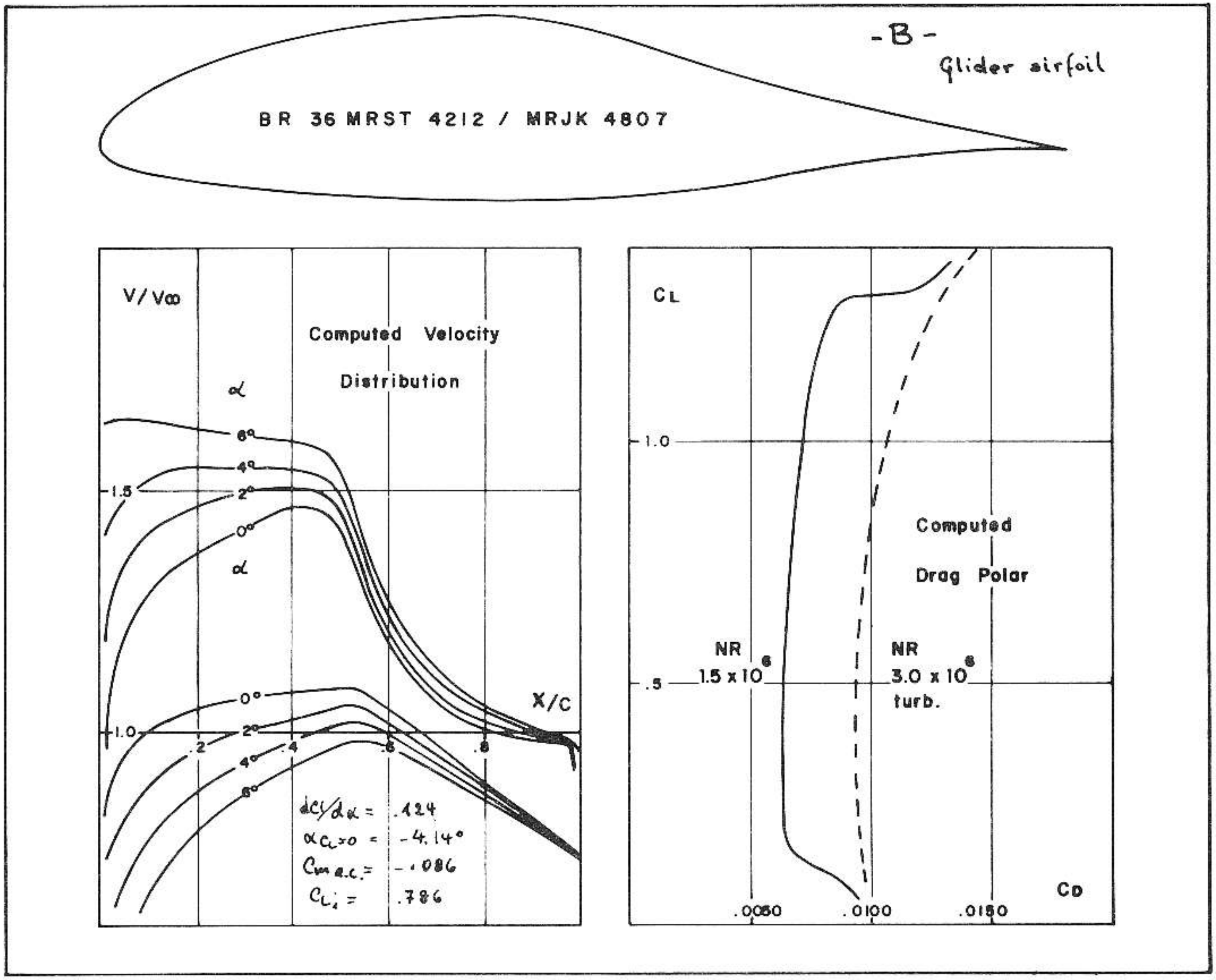

B - AIRFOIL 36MRST4212/MRJK4807

FOR GLIDERS

UPPER SURFACE		UNDER SURFACE	
0.1149	1.2975		
0.9619	2.7011	1.6361	-1.2416
2.4753	4.1794	3.4881	-1.8044
4.6320	5.7083	6.0305	-2.3552
7.4118	7.2506	9.2460	-2.8940
10.7926	8.7557	13.1131	-3.4089
14.7478	10.1643	17.5961	-3.8811
19.2464	11.4168	22.6681	-4.2895
24.2523	12.4611	28.2892	-4.6164
29.7249	13.2571	34.4182	-4.8503
35.6194	13.7742	41.0100	-4.9847
41.8682	13.9627	48.0162	-5.0020
44.9238	13.7397	50.6771	-4.8476
48.0841	13.2099	53.4493	-4.8021
51.3416	12.4372	56.3126	-4.5751
54.6698	11.4927	59.2458	-4.2779
61.4324	9.3657	65.2348	-3.5253
68.1673	7.2869	71.2377	-2.6552
74.6780	5.5002	77.0729	-1.7801
80.7753	4.0510	82.5616	-1.0002
86.2787	2.8801	87.5335	-0.3915
91.0230	1.9161	91.8329	+0.0039
94.8648	1.1264	95.3242	+0.1827
97.6981	0.5236	97.8971	+0.1826

Osculatory leading edge radius = 1.6157

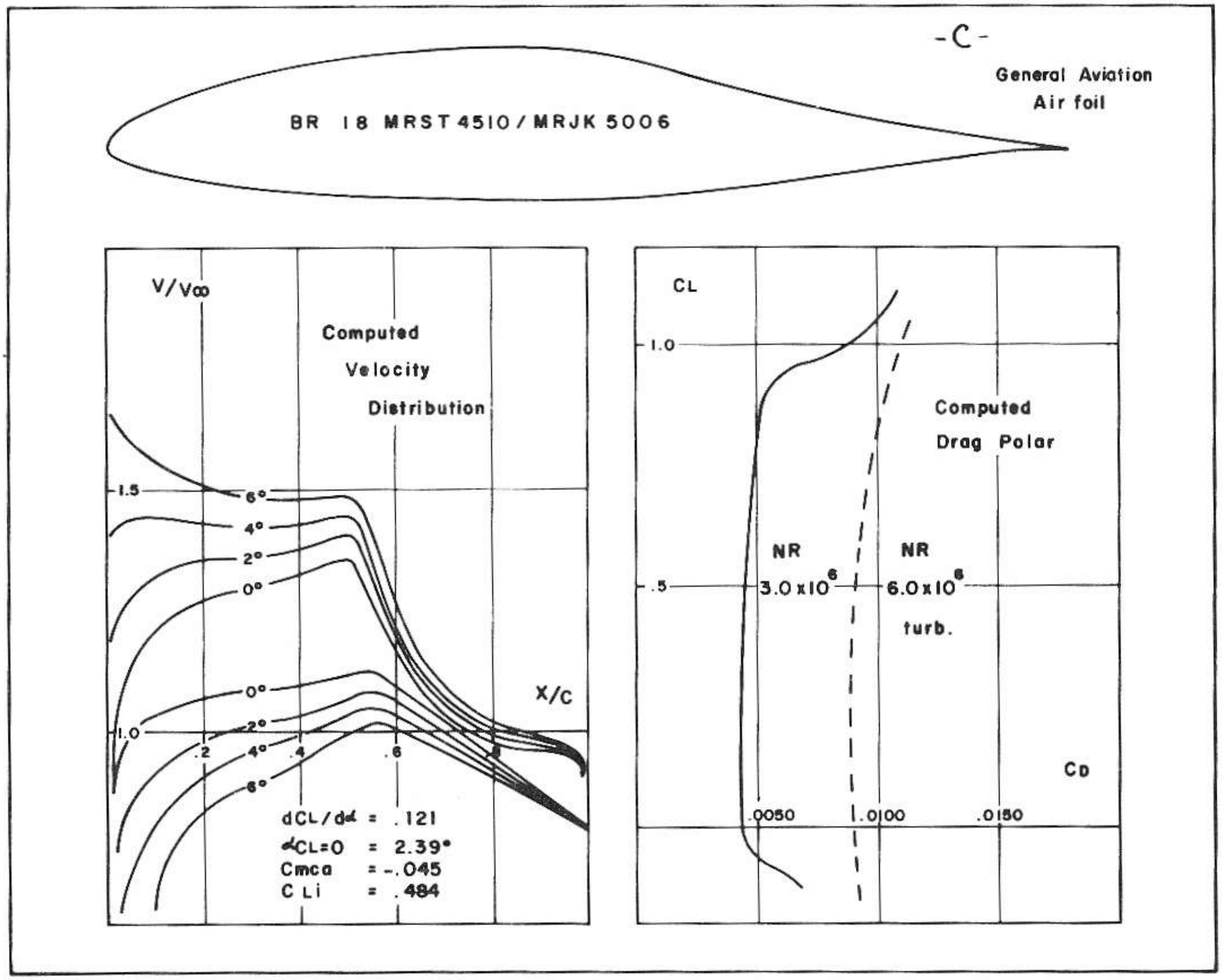

C - AIRFOIL 18MRST4510
FOR GENERAL AVIATION

UPPER SURFACE		UNDER SURFACE	
0.2574	1.0730		
1.2377	2.2032	1.5950	-1.1459
2.9081	3.3805	3.4996	-1.6953
5.2509	4.5908	6.1327	-2.2433
8.2468	5.8071	9.4751	-2.7853
11.8725	6.9903	13.5018	-3.3074
16.1002	8.0938	18.1823	-3.7898
20.8972	9.0703	23.4811	-4.2118
26.2263	9.8785	29.3583	-4.5553
32.0455	10.4869	35.7700	-4.8081
38 3104	10.8716	42.6678	-4.9621
44.9710	10.9929	50.0000	-4.9998
47.6251	10.7939	52.5851	-4.9569
50.7969	10.3430	55.2482	-4.8325
53.8626	9.6941	58.0131	-4.6346
56.9983	8.9067	60.8443	-4.3726
63.3822	7.1487	66.6205	-3.7001
69.7553	5.4516	72.4025	-2.9091
75.9273	4.0179	78.0150	-2.0963
81.7140	2.8838	83.2869	-1.3493
86.9414	1.9961	88.0564	-0.7366
91.4513	1.2903	92.1768	-0.2990
95.1068	0.7324	95.5205	-0.0458
97.7981	0.3241	97.9844	+0.0469

Osculatory leading edge radius = 1.0854

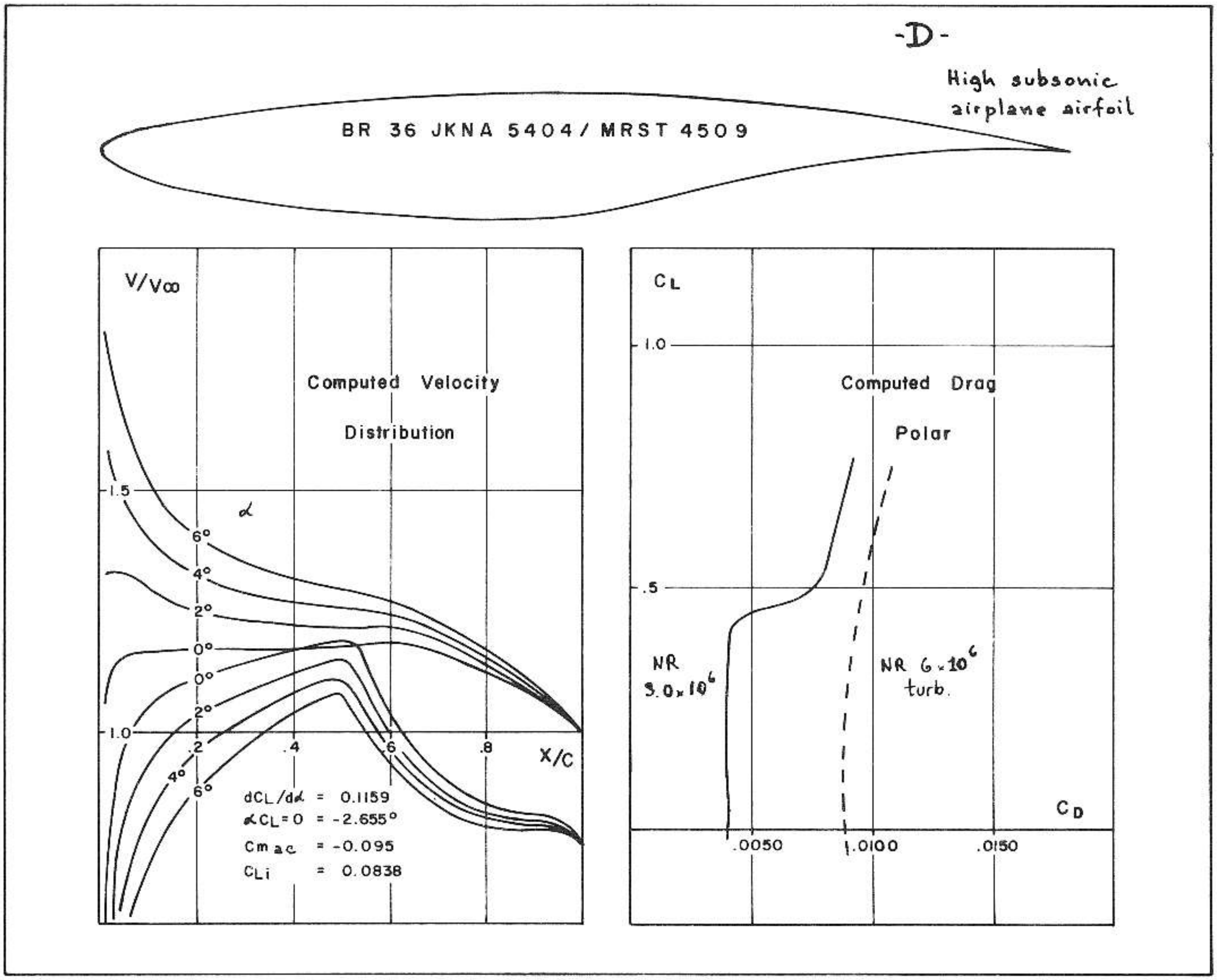

D - AIRFOIL 36JKNA5404/MRST4509

FOR HIGH SUBSONIC AIRPLANE

UPPER SURFACE		UNDER SURFACE	
0.3272	0.6061		
1.5162	1.2995	1.5992	-1.6698
3.5330	2.0148	3.3511	-2.4584
6.3566	2.7319	5.7450	-3.2393
9.9627	3.4215	8.7656	-4.0076
14.3221	4.0621	12.3906	-4.7439
19.4004	4.6354	16.5931	-5.4199
25.1779	5.1250	21.3417	-6.0054
31.5498	5.5170	26.6017	-6.4744
38.5269	5.7990	32.3350	-6.8089
46.0356	5.9604	38.5000	-6.9974
54.0185	5.9910	45.0521	-7.0140
57.8695	5.9470	50.7849	-6.4088
61.7200	5.7975	56.9085	-5.1562
65.5681	5.5403	63.2453	-3.6835
69.4136	5.1875	69.6017	-2.3388
73.2559	4.7555	75.7783	-1.3029
80.9279	3.6918	81.5815	-0.6005
84.7575	3.0746	86.8317	-0.1705
88.5815	2.4130	91.3832	+0.0637
92.3999	1.7080	95.0531	+0.1618
96.2106	0.9404	97.7720	+0.1532
100.0000	0.0172	100.0000	0.0000

Obsculatory leading edge radius = 0.7301

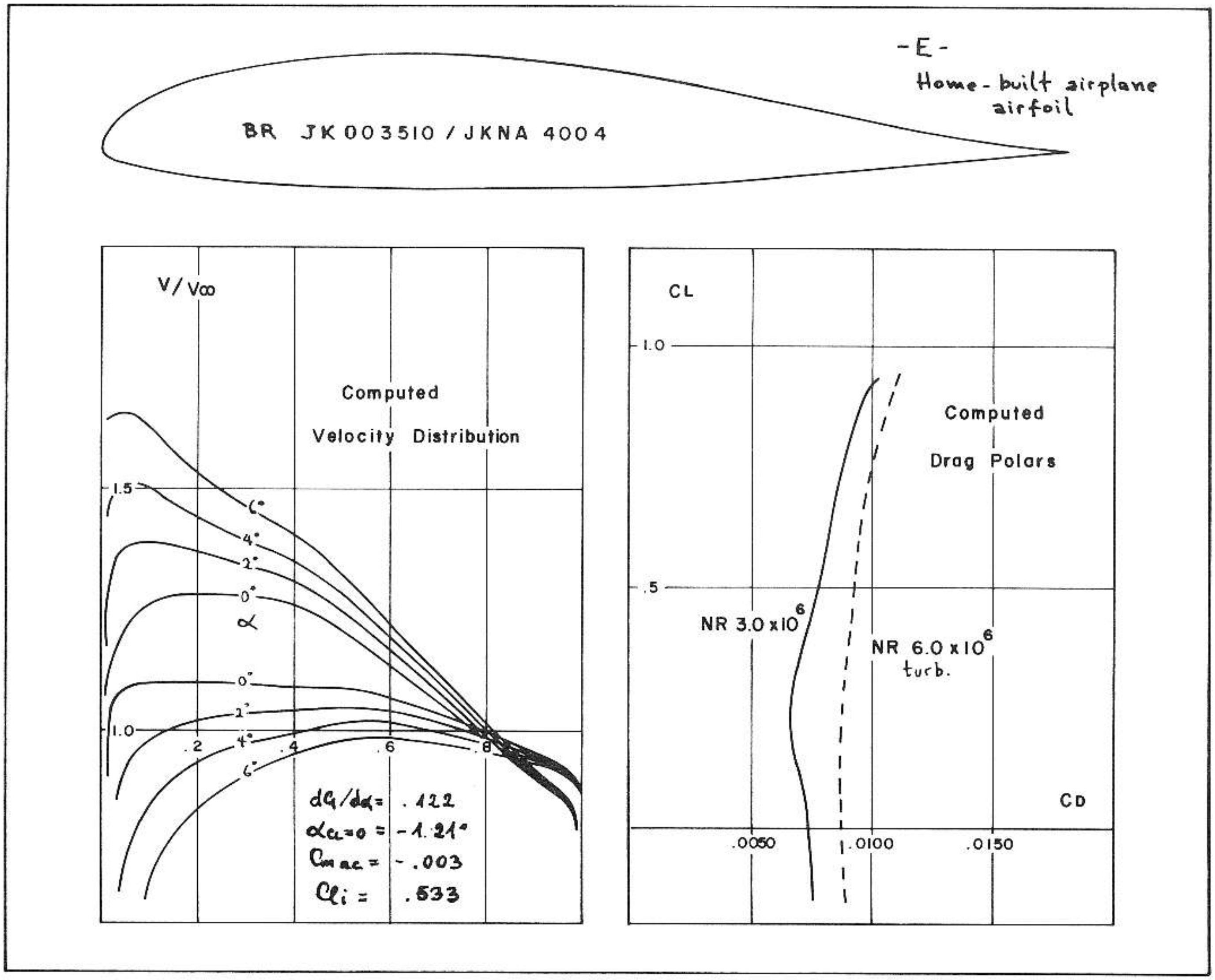

E - AIRFOIL 00JK3510/JKNA4004
FOR HOME-BUILD AIRPLANE

UPPER SURFACE		UNDER SURFACE	
0.266	1.339		
1.063	2.653	1.215	-1.061
2.385	3.917	2.726	-1.567
4.222	5.107	4.825	-2.043
6.558	6.202	7.495	-2.481
9.378	7.182	10.718	-2.873
12.659	8.032	14.468	-3.213
16.377	8.739	18.716	-3.495
20.503	9.292	23.431	-3.717
25.005	9.688	28.577	-3.875
29.850	9.923	34.114	-3.969
35.000	10.000	40.000	-4.000
38.353	9.925	45.000	-3.982
41.846	9.708	50.000	-3.877
45.451	9.360	55.000	-3.682
49.142	8.897	60.000	-3.410
56.667	7.698	65.000	-3.078
64.191	6.265	70.000	-2.700
71.488	4.760	75.000	-2.284
78.333	3.333	80.000	-1.840
84.521	2.106	85.000	-1.386
89.861	1.158	90.000	-0.930
94.194	0.516	95.000	-0.473
97.387	0.159	100.000	-0.017

Osculatory leading edge radius = 1.7248

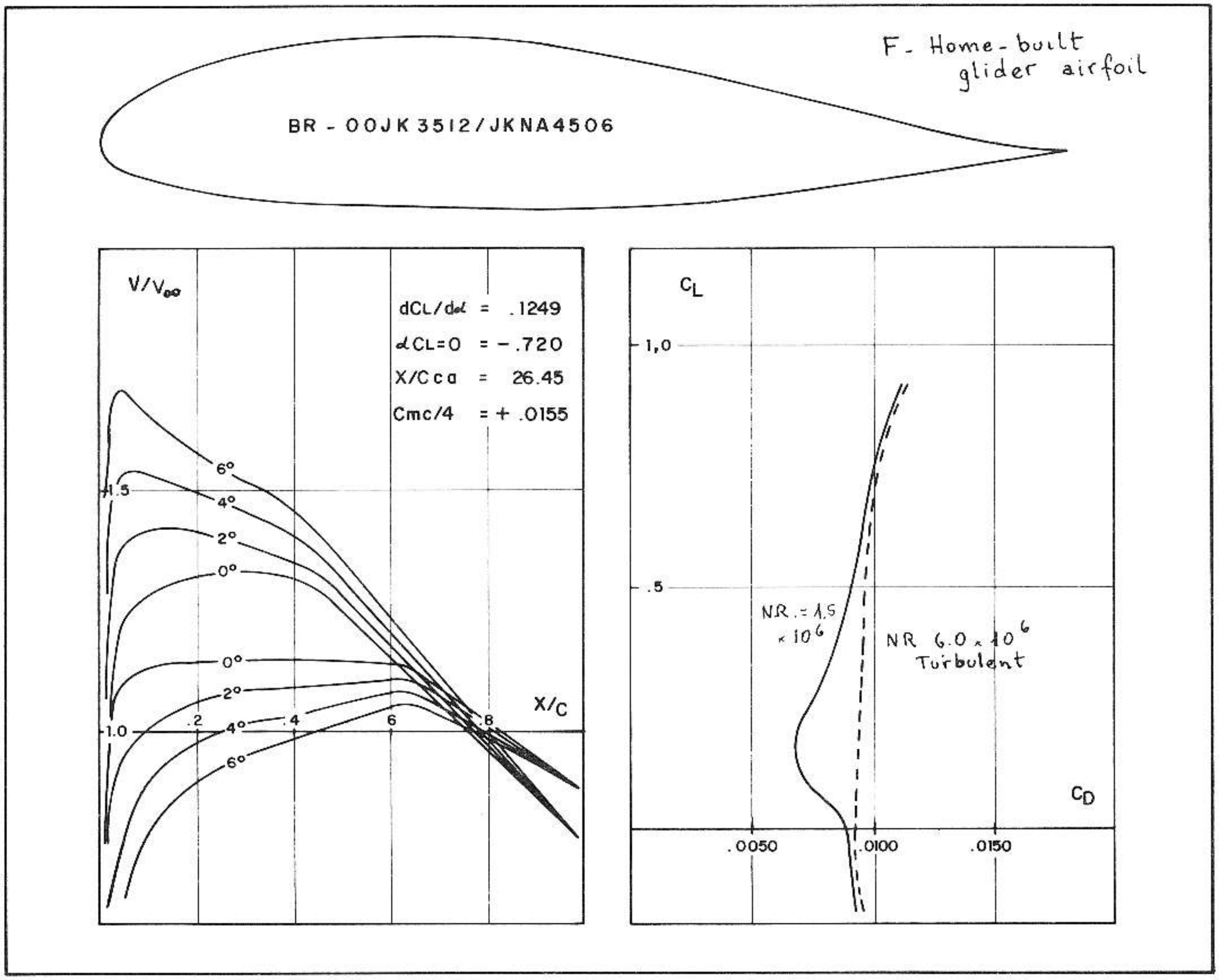

F - AIRFOIL 18JK3512/JKNA4004

FOR AMATEUR BUILT GLIDER

UPPER SURFACE		UNDER SURFACE	
.129	1.628		
.856	3.262	1.283	-0.964
2.194	4.856	2.807	-1.384
3.946	6.375	4.912	-1.762
6.273	7.786	7.585	-2.095
9.096	9.069	10.806	-2.380
12.391	10.183	14.550	-2.615
16.130	11.127	18.790	-2.799
20.285	11.881	23.495	-2.931
24.821	12.435	28.628	-3.011
29.703	12.786	34.152	-3.043
34.893	12.934	40.023	-3.029
38.272	12.871	45.011	-2.989
41.790	12.630	50.000	-2.877
45.422	12.226	54.989	-2.689
49.137	11.677	59.980	-2.438
56.702	10.225	64.973	-2.144
64.255	8.458	69.967	-1.819
71.563	6.574	74.964	-1.472
78.408	4.759	79.860	-1.118
84.589	3.149	84.965	-0.775
89.906	1.862	89.970	-0.460
94.219	0.938	94.381	-0.161
97.397	0.365	100.000	-0.017

Osculatory leading edge radius = 2.2528